

ImplicitDeepfake: Plausible Face-Swapping through Implicit Deepfake Generation using NeRF and Gaussian Splatting

Georgii Stanishevskii^{1*}, Jakub Steczkiewicz^{1*}, Tomasz Szczepanik^{1*},
Sławomir Tadeja², Jacek Tabor¹, Przemysław Spurek¹

*Equal contribution

¹Jagiellonian University, Faculty of Mathematics and Computer Science, Cracow, Poland

²Department of Engineering, University of Cambridge, Cambridge, UK
przemyslaw.spurek@uj.edu.pl

Abstract

Numerous emerging deep-learning techniques have had a substantial impact on computer graphics. Among the most promising breakthroughs are the recent rise of Neural Radiance Fields (NeRFs) and Gaussian Splatting (GS). NeRFs encode the object’s shape and color in neural network weights using a handful of images with known camera positions to generate novel views. In contrast, GS provides accelerated training and inference without a decrease in rendering quality by encoding the object’s characteristics in a collection of Gaussian distributions. These two techniques have found many use cases in spatial computing and other domains. On the other hand, the emergence of deepfake methods has sparked considerable controversy. Such techniques can have a form of artificial intelligence-generated videos that closely mimic authentic footage. Using generative models, they can modify facial features, enabling the creation of altered identities or facial expressions that exhibit a remarkably realistic appearance to a real person. Despite these controversies, deepfake can offer a next-generation solution for avatar creation and gaming when of desirable quality. To that end, we show how to combine all these emerging technologies to obtain a more plausible outcome. Our *ImplicitDeepfake*¹ uses the classical deepfake algorithm to modify all training images separately and then train NeRF and GS on modified faces. Such relatively simple strategies can produce plausible 3D deepfake-based avatars.

1 Introduction

Manipulating images and videos of human avatars has a long history and spikes many controversies (Zhang, 2022). Moreover, a number of dedicated to this task software tools and packages like Adobe Photoshop² or Adobe Lightroom³ have

¹The source code is available at: <https://github.com/quereste/implicit-deepfake>

²<https://www.adobe.com/products/photoshop.html>

³<https://www.adobe.com/products/photoshop-lightroom.html>

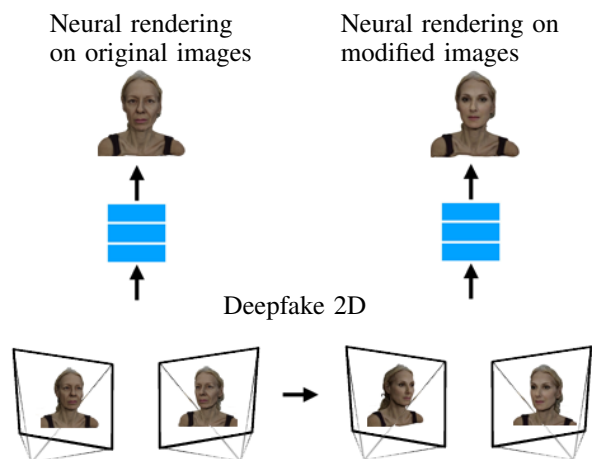


Figure 1: Thanks to neural rendering, we are able to aggregate information from 2D images to produce novel views of 3D objects (see left-hand column). In *ImplicitDeepfake*, we use 2D deepfake on 2D images, and then we use neural rendering to obtain 3D deepfake (see right-hand column).

been developed and become commercially available (Maarek *et al.*, 2021). In this context, realistic facial feature modification that allows for a convincing avatar creation, i.e. resembling someone else appearance to a great extent, remains a non-trivial task that can be supported with emerging deepfake technology (Waseem *et al.*, 2023).

The deepfake term is a combination of *deep learning* and *fake* referring to manipulated media content created using machine learning and artificial neural networks (Waseem *et al.*, 2023). Various deepfake methods employ deep generative models like autoencoders (Tewari *et al.*, 2018) or generative adversarial networks (GAN) (Kumar *et al.*, 2020) for examining the facial characteristics and mimics of a given individual. Such analyses enable the creation of manipulated facial pictures that imitate comparable expressions and motions (Pan *et al.*, 2020).

The availability of user-friendly tools, including DeepFaceLab (Liu *et al.*, 2023), smartphone applications such as

Zao⁴ and FakeApp⁵ has simplified the use and fostered adoption of deepfake by nonprofessionals helping them to swap faces with any target person seamlessly for any desired purpose. Deepfake generation and detection are characterised by intense competition, with defenders (i.e., detectors) and adversaries (i.e. generators) continuously trying to outdo each other. A range of notable advances have been made in both areas in recent years (Turek, 2019).

To extend this growing body of research, we present in this paper *ImplicitDeepfake* a first model that produces a 3D deepfake. To obtain real world 3D objects, we use novel, state-of-the-art machine learning-based methods such as *Neural Radiance Fields* (NeRFs) (Mildenhall *et al.*, 2020) and *Gaussian Splatting* (GS) (Kerbl *et al.*, 2023).



Figure 2: In our paper, we present *ImplicitDeepfake* train on GS and NeRF. As we can see, both models give similar results, with the former producing slightly better deepfakes.

The NeRF concept, first introduced by (Mildenhall *et al.*, 2020), offers a unique approach for generating new views of intricate scenes from a limited set of 2D images with documented camera positional coordinates. NeRFs can create detailed and complex scenes from new perspectives by combining input images and established computer graphics techniques. The strength of NeRF lies in its capacity to extract information from 2D images and camera positions to reconstruct fully-formed 3D objects. It is worth mentioning that the network incorporates the 3D structure, color, shape, and texture of the face into its weights. After training, the network is capable of generating 2D views from any imaginable viewpoint.

The GS (Kerbl *et al.*, 2023) emerges as a compelling alternative for high-quality 3D scene rendering, exhibiting comparable visual fidelity to existing methods while achieving significantly faster inference and training times. This efficiency stems from the lightweight representation of 3D objects as a collection of Gaussian distributions acting like efficient proxies for traditional meshes.

These rendering methods, i.e. NeRFs and GS, can be considered converters from 2D to 3D objects. At the input, we

provide 2D images with viewing positions, and as output, we can obtain 3D objects. In the context of 3D deepfake, we can use a classical model dedicated to 2D images to produce input to the NeRF-based model. *ImplicitDeepfake* apply 2D deepfake for all 2D images separately and then add to NeRF architecture (see Fig. 1). In practice, deepfake technology produces consistent image swapping, and we can directly use natural rendering to produce 3D faces. This solution is universal and can be used with many different approaches based on NeRF or (GS) (Kerbl *et al.*, 2023).

The contributions of our paper can be summarized as follows:

- We propose a new method dubbed *ImplicitDeepfake* which combines neural rendering procedure with 3D deepfake technology.
- We show that *ImplicitDeepfake* can produce consistent face swapping, which allows a direct application of neural rendering on the deepfake output.
- The 2D deepfake produces consistent images, which can be combined with NeRF and GS (see Fig. 2).

2 Related Works

Here, we will discuss various methods proposed for face swapping in images and videos. In most cases, authors use large generative models like autoencoders (Tewari *et al.*, 2018) and generative adversarial networks (GAN) (Kumar *et al.*, 2020). Typically, performing a face swap involves three primary stages (Waseem *et al.*, 2023). Firstly, the algorithm identifies faces in both the source and target videos. Subsequently, the method substitutes the target face’s nose, mouth, and eyes with the corresponding features from the source face. The color and lighting of the candidate’s facial image are modified to ensure a smooth integration of the two faces. Finally, the overlapping region undergoes match distance computation to assess and rank the quality of the merged candidate replacement.

Initially, classical convolutional neural networks (CNNs) were employed for generating deep fakes (Korshunova *et al.*, 2017). However, these methods are limited, as they can only transform individual images and are unsuitable for creating high-quality videos.

In contrast, Reddit⁶ introduced a deepfake video creation method that employs an autoencoder architecture. This approach involves a deepfake face-swapping autoencoder network consisting of one encoder and two decoders. Throughout the training phase, the encoder and the two decoders share parameters. Such autoencoder-based technique is utilized by different face-swapping applications, including *DeepFaceLab* (Liu *et al.*, 2023) and *DFaker*⁷.

The next generative models used in deepfake were generative adversarial networks (GANs). For example, the *FaceSwap GAN* (FS-GAN) utilizes an encoder-decoder architecture as its generator, along with antagonistic and perceptive losses, to enhance the automated coding system. Including

⁴<https://zaodownload.com>

⁵<https://www.malavida.com/en/soft/fakeapp/>

⁶<https://www.reddit.com/r/deepfakes/>

⁷<https://github.com/dfaker/df>

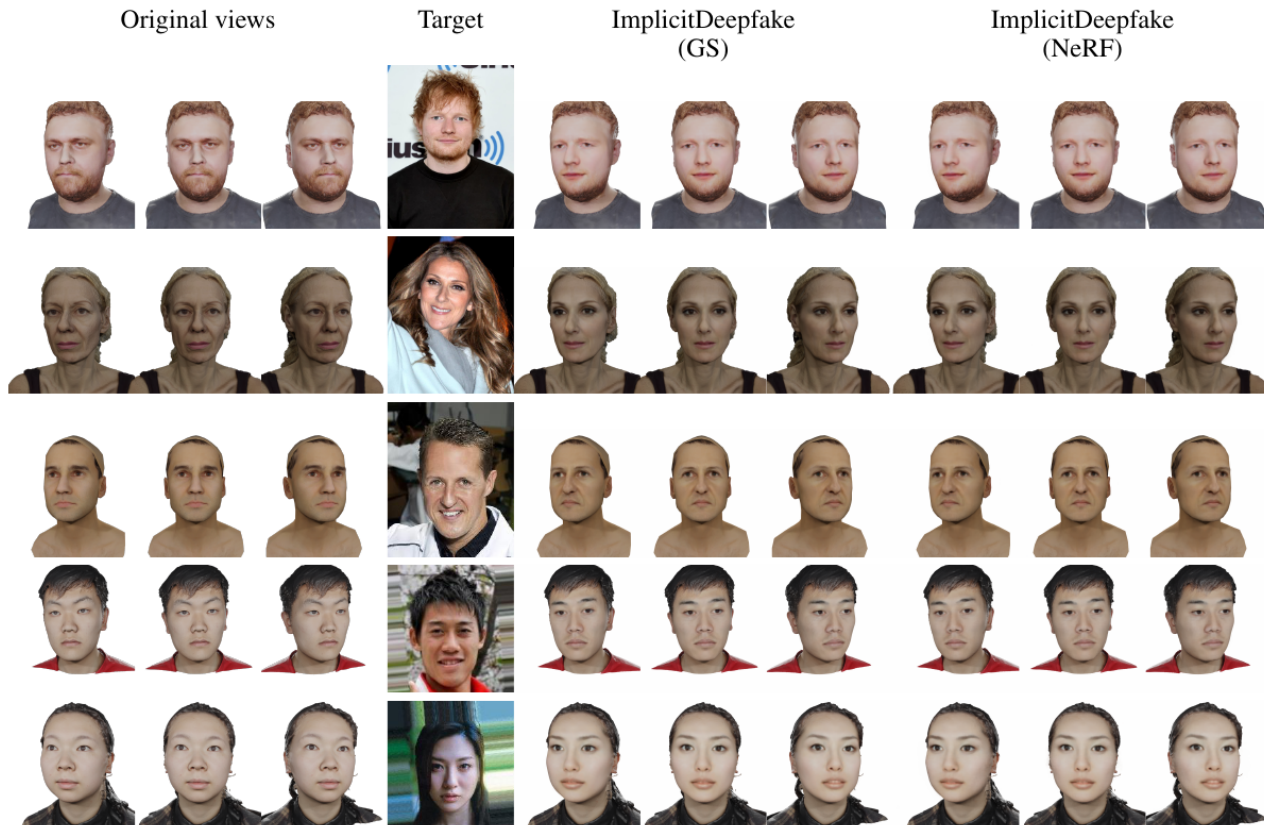


Figure 3: Comparison between ImplicitDeepfake train on GS and NeRF, respectively. In the first column, we see the original input 3D avatars. Then, we present an image of the target celebrity for deepfake. In the last two columns, we present the results obtained with the help of GS and NeRF. As we can observe, GS generally provides more visually plausible renders.

counter losses has improved image reconstruction efficiency while using perceptual loss has helped align the generated face with the input image. On the other hand, the RSGAN (Natsume *et al.*, 2018) utilizes two variational autoencoders (VAE) to produce distinct latent vector embeddings for hair and face areas. These embeddings are subsequently merged to generate a face that has been swapped.

FSNet (Natsume *et al.*, 2019) simplifies the pre- and post-processing phases by removing their complexity. FSNet consists of two sub-networks: a VAE, which produces the latent vector for the face region in the source image, and a generator network, which combines the latent vector of the source face with the non-face components, such as hairstyles and backgrounds of the target image, thereby achieving face swapping.

The FaceShifter approach (Li *et al.*, 2019) employs a two-step approach. Initially, a GAN network is utilized to extract and flexibly merge the identities of the source and target images. Subsequently, the occluded regions are refined using the Heuristic Error Acknowledging Refinement Network (HEAR). In the study conducted by Xu *et al.* (2022), StyleGAN is employed to separate facial image’s texture and appearance characteristics. This technique allows for the preservation of desired target look and texture while maintaining the source identity.

Aside from the discussed examples, there exist many dif-

ferent approaches in the literature and on many GitHub pages. Thus, it is not achievable to verify all existing methods in a practical manner. As such, we decided to use GHOST (Groshv *et al.*, 2022) during our experiments. To our knowledge, ImplicitDeepfake is the first model that utilizes the NeRF and GS approach for generating 3D deepfakes.

3 Method

Here, we describe our ImplicitDeepfake model. First, we introduce both the NeRF and GS and establish a notation. Then, we describe a deepfake model used in our approach. Finally, we present our model.

3.1 Neural Radiance Field (NeRF)

The vanilla NeRF model proposed in Mildenhall *et al.* (2020) is a neural architecture used to represent 3D scenes. In NeRF, a 5-dimensional coordinate is taken as input, consisting of the spatial location $\mathbf{x} = (x, y, z)$ and the viewing direction $\mathbf{d} = (\theta, \psi)$. The model then outputs the emitted color $\mathbf{c} = (r, g, b)$ and the volume density σ .

A classical NeRF model utilizes a set of images during the training process. This approach generates a group of rays, which pass through the image. Neural networks predict color and depth information on such rays to represent a 3D object.

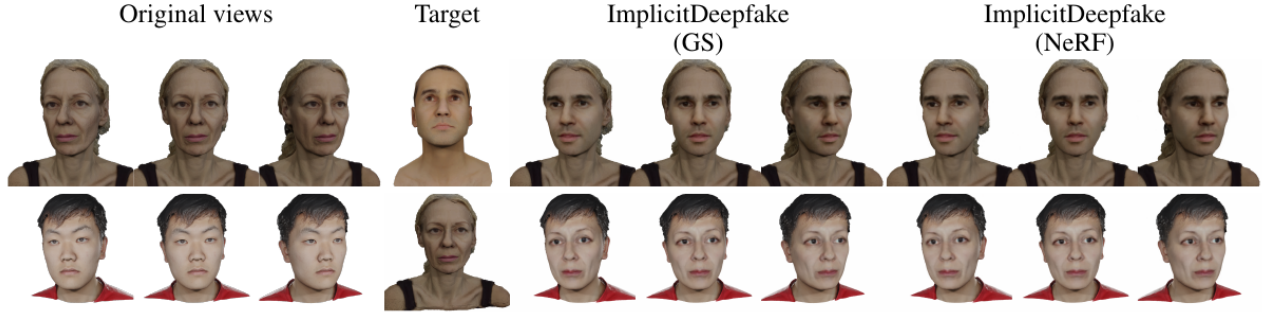


Figure 4: Comparison between ImplicitDeepfake train on GS and NeRF, respectively. In the first column, we see the original input 3D avatars. Then, we present an image of the target avatar (in training, we use only a single image) for deepfake. In the last two columns, we show the results obtained with the help of GS and NeRF.

NeRF encodes such 3D objects using a Multilayer Perceptron (MLP) network:

$$\mathcal{F}_{NeRF}(\mathbf{x}, \mathbf{d}; \Theta) = (\mathbf{c}, \sigma).$$

The training process involves optimizing the parameters (Θ) of the multilayer perceptron (MLP) to minimize the difference between the rendered and reference images obtained from a specific dataset. This calibration allows the MLP network to take in a 3D coordinate and its corresponding viewing direction as input and produce a density value and color (radiance) along that direction.

The loss function of NeRF is inspired by the classical volume rendering Kajiya and Von Herzen (1984). It involves tracing the paths of individual light rays through the scene geometry and calculating their final color. The loss function, used to quantify the discrepancy between the rendered and ground truth pixel colors, is formulated as the sum of squared errors between the corresponding color values in the following manner:

$$\mathcal{L} = \sum_{\mathbf{r} \in R} \|\hat{C}(\mathbf{r}) - C(\mathbf{r})\|_2^2,$$

where R is the set of rays in each batch, $C(\mathbf{r})$ is the ground truth red-green-blue (RGB) color, and $\hat{C}(\mathbf{r})$ is predicted RGB colors for a given ray \mathbf{r} . The predicted RGB colors $\hat{C}(\mathbf{r})$ can be calculated thanks to this formula:

$$\hat{C}(\mathbf{r}) = \sum_{i=1}^N T_i (1 - \exp(-\sigma_i \delta_i)) \mathbf{c}_i,$$

where $T_i = \exp\left(-\sum_{j=1}^{i-1} \sigma_j \delta_j\right)$ and N denotes the number of samples, δ_i is adjacent samples distance, and σ_i is the opacity of a given sample i . This function for calculating $\hat{C}(\mathbf{r})$ from the set of (c_i, σ_i) values is trivially differentiable.

The NeRF’s performance limitations can be attributed to two primary factors, i.e., the inherent capacity constraints of the underlying neural network and the computational difficulty of accurately computing the intersection points between camera rays and the scene geometry. These limitations can lead to prolonged rendering times for high-resolution images, particularly for complex scenes, impeding the potential of real-time applications.

3.2 Gaussian Splatting (GS)

The GS model employs a collection of 3D Gaussian functions to represent a 3D scene. Each Gaussian is characterized by a set of parameters, i.e., its position (mean) specifying its center, its covariance matrix defining the shape and orientation of the Gaussian distribution, its opacity controlling the level of transparency, and its color represented by spherical harmonics (SH) (Fridovich-Keil *et al.*, 2022; Müller *et al.*, 2022).

The GS represents a radiance field by optimizing all the 3D Gaussian parameters. Moreover, the computational efficiency of the GS algorithm stems from its rendering process, which leverages the projection properties of Gaussian components. This approach relies on representing the scene with a dense set of 3D Gaussians, mathematically denoted as:

$$\mathcal{G} = \{(\mathcal{N}(\mathbf{m}_i, \Sigma_i), \sigma_i, c_i)\}_{i=1}^n,$$

where \mathbf{m}_i is the position, Σ_i denotes the covariance, σ_i is the opacity, and c_i are the i -th component’s SH for color representation.

The GS optimization algorithm operates through an iterative image synthesis process and comparison with training views. The challenges of this procedure arise due to potential inaccuracies in Gaussian component placement stemming from the inherent dimensionality reduction of 3D to 2D projection. To mitigate these issues, the algorithm incorporates mechanisms for creating, removing, and relocating Gaussian components. Notably, the precision of 3D Gaussian covariance parameters proves paramount in ensuring a compact data representation. This is attributed to their ability to effectively model large homogeneous regions with a limited number of large anisotropic Gaussians.

GS begins with a finite set of points and proceeds by implementing a strategy of generating fresh elements and removing redundant ones. After every one hundred iterations, the algorithm eliminates any Gaussians that possess an opacity below a predetermined threshold. Concurrently, novel Gaussian components are introduced within unoccupied regions of the 3D space to progressively fill vacant areas and refine the scene representation. Despite the GS optimization procedure’s inherent complexity, implementing the algorithm using CUDA kernels facilitates highly efficient training. This enables GS

	PSNR \uparrow								
	FACE 1	FACE 2	FACE 3	FACE 4	FACE 5	FACE 6	FACE 7	FACE 8	Avg.
NeRF	37.89	38.58	37.95	41.01	36.86	37.77	35.91	35.14	37.64
Gaussian Splatting	41.58	41.71	42.45	44.00	41.25	41.73	39.65	41.43	41.73
	SSIM \uparrow								
NeRF	0.97	0.97	0.98	0.99	0.98	0.98	0.98	0.97	0.98
Gaussian Splatting	0.99	0.99	0.99	0.99	0.99	1.00	0.99	0.99	0.99
	LPIPS \downarrow								
NeRF	0.08	0.08	0.07	0.06	0.04	0.04	0.05	0.06	0.06
Gaussian Splatting	0.04	0.04	0.03	0.03	0.02	0.01	0.02	0.02	0.03

Table 1: Comparison between deepfake on test positions (camera position that is not used in training of ImplicitDeepfake) obtained by ImplicitDeepfake and direct application of deepfake. Results are calculated using faces from Fig. 3.

to achieve comparable quality to NeRF while potentially exhibiting faster training and inference times.

3.3 Deepfake with GHOST

Numerous deepfake technologies have been developed in the literature, each with its own set of limitations. These may include errors in face edge detection, inconsistencies in eye gaze, and overall low quality, particularly when replacing a face from a single image with a video (Waseem *et al.*, 2023). An example approach to deepfake is represented by Generative High-fidelity One Shot Transfer (GHOST) (Groshev *et al.*, 2022), in which the authors build on the FaceShifter (Li *et al.*, 2019) model as a starting point and introduce several enhancements in both the quality and stability of deepfake. Consequently, we decided to utilize GHOST (Groshev *et al.*, 2022) as a deepfake component of our model.

Let I_s and I_t be the cropped faces from the source and target images, respectively, and let $\hat{I}_{s,t}$ be the newly generated face. The architecture of GHOST (Groshev *et al.*, 2022) consists of a few main parts. The identity encoder extracts information from the source image I_s and keeps information about the identity of the source person. The attribute encoder is a model with a U-Net (Ronneberger *et al.*, 2015).

The AAD generator is a model that combines the attribute vector obtained from I_t and the identity vector obtained successively from I_s using AAD ResBlocks. This process generates a new face $\hat{I}_{s,t}$ that possesses the attributes of both the source identity and the target. Moreover, using a multiscale discriminator (Park *et al.*, 2019) improves the quality of the output synthesis by comparing genuine and fake images.

The GHOST model uses the cost function consisting of a few elements representing reconstruction, attributes, identity, and the GAN loss based on a multi-scale discriminator. Once a model has been trained, it can replace a person’s face in one image with the face from another image. However, since the model is trained explicitly on cropped faces, it cannot be directly applied to any images. To utilize the model, it is necessary to first crop the faces from both the source and target images. Once this step is completed, the model can swap the faces in the cropped images. Finally, the result of the face swap is inserted back into the original target image.

The primary issue with this procedure is that the attributes of I_t on $\hat{I}_{s,t}$ are not identical. Therefore, if we were to insert

$\hat{I}_{s,t}$ directly back into the target image, we could see the edges of such an operation. To solve such problems, GHOST first blends the model’s output $\hat{I}_{s,t}$ with I_t , then inserts the result into the target image.

Such a procedure is complicated since we need to crop images. But in the context of neural rendering, applying in the second stage is crucial. The main problem with applying NeRF to modified images is the consistency of the scene. In the case of NeRF inpainting, when we apply the 2D algorithm separately, we obtain inconsistent images, and the NeRF component cannot be trained (Mirzaei *et al.*, 2023). To solve this problem, we must train the inpainting component with the NeRF model simultaneously (Shen *et al.*, 2024).

Our approach takes the main face shape from the source image and changes only the cropped part. Therefore, we can use deepfake and neural rendering components separately.

3.4 ImplicitDeepfake

Our model is a hybrid of the classical deepfake model and neural rendering that can use either NeRF or GS models. In general, we can rely on any other approach to produce novel views from 2D images.

To unify the notation, we will treat the neural rendering model as a black box that takes a set of images with camera positions:

$$\mathcal{I} = \{(I_i, \mathbf{d}_i)\}_{i=1}^k,$$

where I_i is a 3D image from training data and \mathbf{d}_i is the camera position of the I_i image.

We define a neural rendering model by the following function:

$$F(\mathbf{d}; \mathcal{I}, \Theta) = I_{\mathbf{d}},$$

that depends on training images \mathcal{I} and parameters Θ that are adjusted during training. In the case of NeRF, this function describes neural network parameters. In contrast, in the case of GS, it describes the parameters of Gaussian components. Our neural rendering process returns image $I_{\mathbf{d}}$ from given position \mathbf{d} .

The deepfake model, we denote by

$$\hat{I}_{s,t} = \mathcal{G}(I_s, I_t; \Phi),$$

where I_s and I_t are the faces of the source and target images, respectively, Φ denote all parameters of the deepfake

	FACE 1	FACE 2	FACE 3	FACE 4	FACE 5	FACE 6	FACE 7	Avg.
PSNR \uparrow								
deepfake 2D	12.75	11.97	13.94	11.35	11.47	12.31	11.84	12.23
NeRF	13.27	12.92	12.18	11.76	12.08	12.91	12.61	12.54
Gaussian Splatting	12.81	12.04	13.86	11.42	11.51	12.33	11.89	12.27
SSIM \uparrow								
deepfake 2D	0.75	0.76	0.74	0.70	0.72	0.75	0.75	0.74
NeRF	0.83	0.83	0.81	0.79	0.82	0.80	0.81	0.81
GS	0.75	0.76	0.75	0.71	0.72	0.75	0.75	0.74
LPIPS \downarrow								
deepfake 2D	0.28	0.27	0.26	0.27	0.25	0.25	0.24	0.26
NeRF	0.26	0.26	0.25	0.26	0.24	0.24	0.24	0.25
GS	0.27	0.27	0.26	0.27	0.25	0.25	0.24	0.26

Table 2: We conduct a comparison using data from two 3D avatars. We select an image from the target avatar and employ it like in the initial experiment. At the same time, we use the remaining views of the target avatar as testing data. In this experiment, we evaluate the outcomes of ImplicitDeepfake compared to the original training views of the target avatar. As a reference point, we utilize a model that directly applies 2D deepfake on the training views of the target avatar.

network, in our case GHOST (Groshev *et al.*, 2022). Our deepfake model returns the newly generated face $\hat{I}_{s,t}$.

The general framework for our ImplicitDeepfake consists of two parts. First, we take training images of the 3D face:

$$\mathcal{I} = \{(I_i, \mathbf{d}_i)\}_{i=1}^k,$$

and target image I_t for the deepfake procedure. Then, we apply the deepfake model separately for all modified images:

$$\hat{\mathcal{I}} = \{\hat{I}_{i,t}\}_{i=1}^k = \{\mathcal{G}(I_i, I_t; \Phi)\}_{i=1}^k.$$

Next, we train neural rendering on modified images to obtain a model dedicated to producing novel views I_d :

$$F(\mathbf{d}; \hat{\mathcal{I}}, \Theta) = I_d.$$

The above procedure is relatively simple and can generate plausible 3D deepfake avatars, as shown in Fig. 3.

4 Experiments

Here, we present the resulting deepfakes produced by our model. We start from a classical approach when we have one target image of a celebrity and the 3D object of a 3D human avatar. We aim to change the latter into an avatar of a celebrity using a target image, as shown in Fig. 3.

In our experiment, we apply classical 2D deepfake on source images. Then, we train our NeRF or GS model on modified images to obtain a 3D avatar of a given celebrity. To evaluate our model, we chose novel views of the source 3D avatar and applied deepfake. Such images were compared with results generated with our ImplicitDeepfake. In Tab. 1, we present a numerical comparison between NeRF and GS is presented. As we can see, GS obtained slightly better results.

In the second experiment, we wanted to contrast our results with the actual images of the target celebrity. Therefore, we used two 3D avatars instead of one. We took a single image from the target avatar and used it like in the first experiment. The other views of the target avatar served as testing data. Due to this, we could compare the results given by our ImplicitDeepfake with the original training views of the target

avatar, as shown in Fig. 4. As a baseline, we used a model that directly applies 3D deepfake to training views of the target avatar. A numerical comparison between NeRF and GS can be seen in Tab. 2. As we can observe, ImplicitDeepfake gives better results than our baseline.

In summary, we can see that applying 2D deepfake constructs well-aligned data. Moreover, independent modification produces consistent views to train both NeRF and GS.

We also can observe that GS gives sharper renders, as seen in Tab. 1. We believe that this difference is caused by NeRF, which occasionally produces blurred renders when the 2D Deepfake model produces inconsistent renders. We can observe that, compared to NeRF, GS is more robust and works with issues related to the classical deepfake algorithm.

5 Conclusions

This paper introduces a novel, *ImplicitDeepfake*, a method that uses the conventional deepfake algorithm to alter the training images for NeRF and GS, respectively. Subsequently, NeRF and GS are trained separately on the modified facial images, generating realistic and plausible deepfakes that can serve as 3D avatars. As shown in the results, GS produces sharper renders, with the former occasionally generating blurred renders. We attribute these effects to minor inconsistencies introduced by the 2D deepfake model. Overall, GS demonstrates greater resilience to view inconsistencies than NeRF.

References

- Sara Fridovich-Keil, Alex Yu, Matthew Tancik, Qinhong Chen, Benjamin Recht, and Angjoo Kanazawa. Plenoxels: Radiance fields without neural networks. In *CVPR*, pages 5501–5510, 2022.
- Alexander Groshev, Anastasia Maltseva, Daniil Chesakov, Andrey Kuznetsov, and Denis Dimitrov. Ghost€: a new face swap approach for image and video domains. *IEEE Access*, 10:83452–83462, 2022.

- James T Kajiya and Brian P Von Herzen. Ray tracing volume densities. *ACM SIGGRAPH computer graphics*, 18(3):165–174, 1984.
- Bernhard Kerbl, Georgios Kopanas, Thomas Leimkühler, and George Drettakis. 3d gaussian splatting for real-time radiance field rendering. *ACM Transactions on Graphics*, 42(4), 2023.
- Iryna Korshunova, Wenzhe Shi, Joni Dambre, and Lucas Theis. Fast face-swap using convolutional neural networks. In *Proceedings of the IEEE international conference on computer vision*, pages 3677–3685, 2017.
- Akash Kumar, Arnav Bhavsar, and Rajesh Verma. Detecting deepfakes with metric learning. In *2020 8th international workshop on biometrics and forensics (IWBF)*, pages 1–6. IEEE, 2020.
- Lingzhi Li, Jianmin Bao, Hao Yang, Dong Chen, and Fang Wen. Faceshifter: Towards high fidelity and occlusion aware face swapping. *arXiv preprint arXiv:1912.13457*, 2019.
- Kunlin Liu, Ivan Perov, Daiheng Gao, Nikolay Chervoniy, Wenbo Zhou, and Weiming Zhang. Deepfacelab: Integrated, flexible and extensible face-swapping framework. *Pattern Recognition*, 141:109628, 2023.
- Phoebe Maares, Sandra Banjac, and Folker Hanusch. The labour of visual authenticity on social media: Exploring producers’ and audiences’ perceptions on instagram. *Poetics*, 84:101502, 2021.
- Ben Mildenhall, Pratul P. Srinivasan, Matthew Tancik, Jonathan T. Barron, Ravi Ramamoorthi, and Ren Ng. Nerf: Representing scenes as neural radiance fields for view synthesis. In *ECCV*, 2020.
- Ashkan Mirzaei, Tristan Aumentado-Armstrong, Konstantinos G Derpanis, Jonathan Kelly, Marcus A Brubaker, Igor Gilitschenski, and Alex Levinstein. Spin-nerf: Multi-view segmentation and perceptual inpainting with neural radiance fields. In *Proceedings of the IEEE/CVF Conference on Computer Vision and Pattern Recognition*, pages 20669–20679, 2023.
- Thomas Müller, Alex Evans, Christoph Schied, and Alexander Keller. Instant neural graphics primitives with a multiresolution hash encoding. *ACM Transactions on Graphics (ToG)*, 41(4):1–15, 2022.
- Ryota Natsume, Tatsuya Yatagawa, and Shigeo Morishima. Rsgan: face swapping and editing using face and hair representation in latent spaces. In *ACM SIGGRAPH 2018 Posters*, pages 1–2. 2018.
- Ryota Natsume, Tatsuya Yatagawa, and Shigeo Morishima. Fsnets: An identity-aware generative model for image-based face swapping. In *Computer Vision—ACCV 2018: 14th Asian Conference on Computer Vision, Perth, Australia, December 2–6, 2018, Revised Selected Papers, Part VI 14*, pages 117–132. Springer, 2019.
- Deng Pan, Lixian Sun, Rui Wang, Xingjian Zhang, and Richard O Sinnott. Deepfake detection through deep learning. In *2020 IEEE/ACM International Conference on Big Data Computing, Applications and Technologies (BD-CAT)*, pages 134–143. IEEE, 2020.
- Taesung Park, Ming-Yu Liu, Ting-Chun Wang, and Jun-Yan Zhu. Semantic image synthesis with spatially-adaptive normalization. In *Proceedings of the IEEE/CVF conference on computer vision and pattern recognition*, pages 2337–2346, 2019.
- Olaf Ronneberger, Philipp Fischer, and Thomas Brox. U-net: Convolutional networks for biomedical image segmentation. In *Medical Image Computing and Computer-Assisted Intervention—MICCAI 2015: 18th International Conference, Munich, Germany, October 5–9, 2015, Proceedings, Part III 18*, pages 234–241. Springer, 2015.
- I-Chao Shen, Hao-Kang Liu, and Bing-Yu Chen. Nerf-in: Free-form nerf inpainting with rgb-d priors. *Computer Graphics and Applications (CG&A)*, 2024.
- Ayush Tewari, Michael Zollhoefer, Florian Bernard, Pablo Garrido, Hyeonwoo Kim, Patrick Perez, and Christian Theobalt. High-fidelity monocular face reconstruction based on an unsupervised model-based face autoencoder. *IEEE transactions on pattern analysis and machine intelligence*, 42(2):357–370, 2018.
- Matt Turek. Media forensics (medifor). *Defense Advanced Research Projects Agency, Defense Advanced Research Projects Agency (DARPA)*, www.darpa.mil/program/media-forensics. Accessed, 10, 2019.
- Saima Waseem, Syed R Abu-Bakar, Bilal Ashfaq Ahmed, Zaid Omar, Taiseer Abdalla Elfadil Eisa, and Mhassen Elneel Dalam. Deepfake on face and expression swap: A review. *IEEE Access*, 2023.
- Yangyang Xu, Bailin Deng, Junle Wang, Yanqing Jing, Jia Pan, and Shengfeng He. High-resolution face swapping via latent semantics disentanglement. In *Proceedings of the IEEE/CVF Conference on Computer Vision and Pattern Recognition*, pages 7642–7651, 2022.
- Tao Zhang. Deepfake generation and detection, a survey. *Multimedia Tools and Applications*, 81(5):6259–6276, 2022.